

Article

One-Pot Synthesis of Stable Poly([c2]Daisy-chain Rotaxane) with Pseudo-Stopper via Metathesis Reaction and Thiol-Ene Reaction

Risako Kamoto, Kenjiro Onimura and Kazuhiro Yamabuki * 

Graduate School of Sciences and Technology for Innovation, Yamaguchi University, 2-16-1 Tokiwadai, Ube 755-8611, Yamaguchi, Japan; onimura@yamaguchi-u.ac.jp (K.O.)

* Correspondence: yamabuki@yamaguchi-u.ac.jp

Abstract: Rotaxanes, known as supramolecular compounds, are expected to find applications in functional materials due to their high degree of freedom. However, their synthesis requires multistep reactions, and there is a demand for more convenient methods to synthesize rotaxane materials. In this study, we aimed to investigate a simpler method for synthesizing highly functional rotaxane materials and explore the diversity of molecular designs. To achieve this, we successfully synthesized a host-guest conjugated compound that incorporates both crown ether as the host unit and secondary ammonium salts as the guest unit within the same molecule. Subsequently, the metathesis reaction of these compounds, which construct [c2]daisy-chain rotaxanes, enabled the one-pot synthesis of a topological polymer called “poly([c2]daisy-chain rotaxane)” with a pseudo-stopper. This methodology achieves the stabilization and polymerization of rotaxanes simultaneously, contributing to the easy materialization of rotaxanes. Furthermore, the thiol-ene reaction achieved the extension of the distance between rotaxane units and provided a useful approach to diversify the design of functional materials with rotaxane structures.

Keywords: [c2]daisy-chain rotaxane; metathesis reaction; thiol-ene reaction



Citation: Kamoto, R.; Onimura, K.; Yamabuki, K. One-Pot Synthesis of Stable Poly([c2]Daisy-chain Rotaxane) with Pseudo-Stopper via Metathesis Reaction and Thiol-Ene Reaction. *Reactions* **2023**, *4*, 448–464. <https://doi.org/10.3390/reactions4030027>

Academic Editor: Vincent Ladmira

Received: 12 July 2023

Revised: 3 August 2023

Accepted: 17 August 2023

Published: 23 August 2023



Copyright: © 2023 by the authors. Licensee MDPI, Basel, Switzerland. This article is an open access article distributed under the terms and conditions of the Creative Commons Attribution (CC BY) license (<https://creativecommons.org/licenses/by/4.0/>).

1. Introduction

Rotaxanes are a well-known type of supramolecular structures that exhibit organized arrangements through interactions between molecules. A rotaxane is a general term for a mechanically interlocked molecule where a linear molecule (known as the “axle”) threads through the cavity of a cyclic molecule (referred to as the “wheel”), and numerous rotaxanes have been reported to date. For instance, Harada et al. have reported a typical rotaxane shaped like a necklace by utilizing hydrophilic cyclodextrins as a host and incorporating an axle such as polyethylene glycol into the cavity [1–11]. These systems take advantage of the complementary sizes and hydrophobic interactions between the host and guest molecules, allowing for the formation of precisely controlled complexes. On the other hand, research on rotaxanes using hydrophobic cyclic molecules, with a focus on Stoddart and Gibson et al.’s work, has been actively reported since the 1990s [12–23]. Through cyclodextrins, various interactions can be utilized for the synthesis of rotaxanes. For example, Stoddart et al. successfully synthesized a rotaxane consisting of a 4,4'-bipyridinium unit and a bisparaphenylene-34-crown-10 macrocycle, utilizing charge-transfer interactions [15]. Gibson et al. found that a 30-membered crown ether forms hydrogen bonds with hydroxyl groups at the polymer chain termini, promoting rotaxane formation [21]. Furthermore, Sauvage et al. reported the synthesis of rotaxanes using the coordination structure of Cu ion and crown ether derivatives with phenanthroline skeleton, establishing an efficient synthesis method utilizing the template effect between a metal ion and a ligand [18]. Additionally, Takata et al. reported the synthesis of hydrophobic functional rotaxanes utilizing hydrogen bonds and electrostatic interactions working between the secondary ammonium salt axles

and the dibenzo-24-crown-8-ether (DB24C8) derivatives [24–26]. They demonstrated the utilization of these rotaxanes not only in small molecules but also in functional polymer materials. Supramolecular compounds utilizing intermolecular interactions, such as rotaxanes, exhibit ordered spatial arrangements and are recognized as artistic compounds. However, in recent years, various functional rotaxane materials with excellent properties, like slide-ring gels, have also gained significant recognition [27–35]. In slide-ring gels, the cyclodextrins within the rotaxane form a hydrogel through intermolecular cross-linking [36]. This hydrogel structure allows the cyclodextrins to freely move along the polyethylene glycol (PEG) axle, effectively mitigating external forces (“Pulley effect”). As a result, these materials exhibit high mechanical strength and stretchability, offering unique functional materials based on a novel concept that distinguishes them from both chemical gels and physical gels. In maintaining the structure and functionality of these rotaxanes, a bulky “stopper” is essential as a third component other than the wheel and axle (Figure 1).

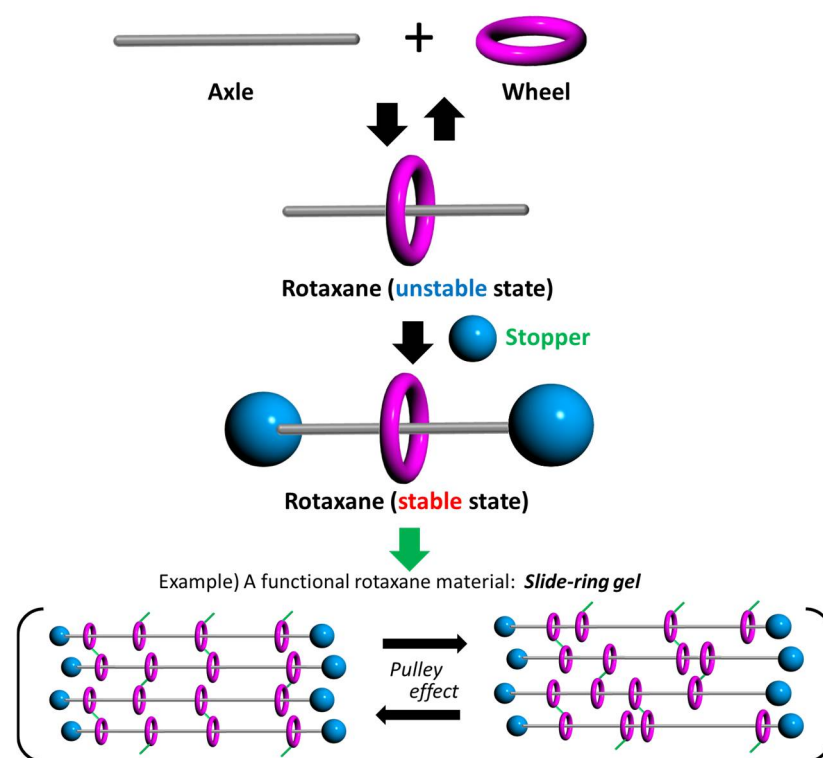


Figure 1. Conventional synthesis method of “rotaxane” and applications of functional rotaxane materials (ex. slide-ring gel).

A “stopper” possesses a size larger than the cavity size of wheel and serves the role of enclosing wheel within the rotaxane. By introducing these bulky compounds at the end of axle, the rotaxane can stably exist without dissociating in various external environments. Therefore, these stoppers are an essential component in the synthesis of many rotaxanes. However, the use of stoppers increases the complexity of the rotaxane synthesis process and leads to lower yields. Therefore, synthesizing rotaxanes efficiently using a simpler method holds significant industrial importance. To address the challenge of simplifying the synthesis of rotaxanes mentioned above, our research group focused on [c2]daisy-chain rotaxanes, which possess a unique structure among rotaxanes [37–62]. [c2]Daisy-chain rotaxanes are constructed from a host–guest connected compound (H-G compound) where the host component (wheel) and the guest component (axle) are incorporated within the same molecule. In these [c2]daisy-chain rotaxanes, two H-G compounds interact with each other, utilizing their wheel and axle components to mutually form an inclusion complex, resulting in a highly symmetrical compound. Such [c2]daisy-chain rotaxanes exhibit changes in the position of their internal wheels only when

stoppers are introduced, in response to external stimuli such as light, pH, temperature, solvent polarity, and mechanical stress. These topological changes enable the creation of new materials with various functionalities such as stimulus responsiveness and stretchability, but there are very few reported examples of such materials [63–70]. Among them, for example, Stoddart et al. reported the synthesis of stable [c2]daisy-chain rotaxanes by introducing a 1,3-Diisopropylbenzene stopper containing an alkyne unit to the host–guest inclusion complex of crown ether and ammonium salt [71]. Furthermore, the rotaxane was successfully polymerized using Huisgen 1,3-dipolar cycloaddition, resulting in the synthesis of a topological polymer “poly([c2]daisy-chain rotaxane)” that allows for precise control of the position of the crown ether. However, this method involves a conventional two-step synthetic approach, where stable rotaxanes are first synthesized and purified using stoppers, followed by polymerization with diazides as joint components. Therefore, a more convenient synthetic approach is desired.

Based on this background, in recent years, we have successfully achieved the one-pot synthesis of a convenient and stable topological material using the [c2]daisy-chain rotaxane structure without employing a third “stopper”. In this study, we report the one-pot synthesis of a polymer composed of continuously linked [c2]daisy-chain rotaxanes using only monoalkene compounds that contain a 24-membered crown ether (wheel) as the host component and a secondary ammonium salt (axle) as the guest component within the same molecule, utilizing metathesis reactions [72–80] (Figure 2).

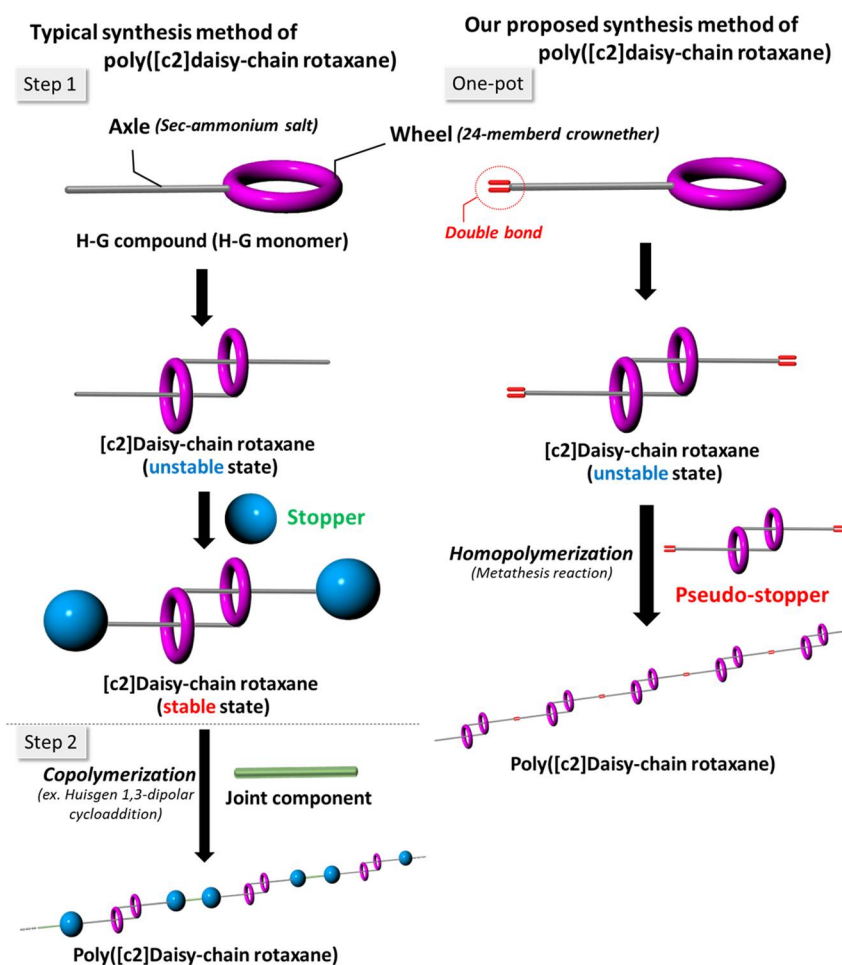


Figure 2. One-pot synthesis of “poly([c2]daisy-chain rotaxane)” with a pseudo-stopper.

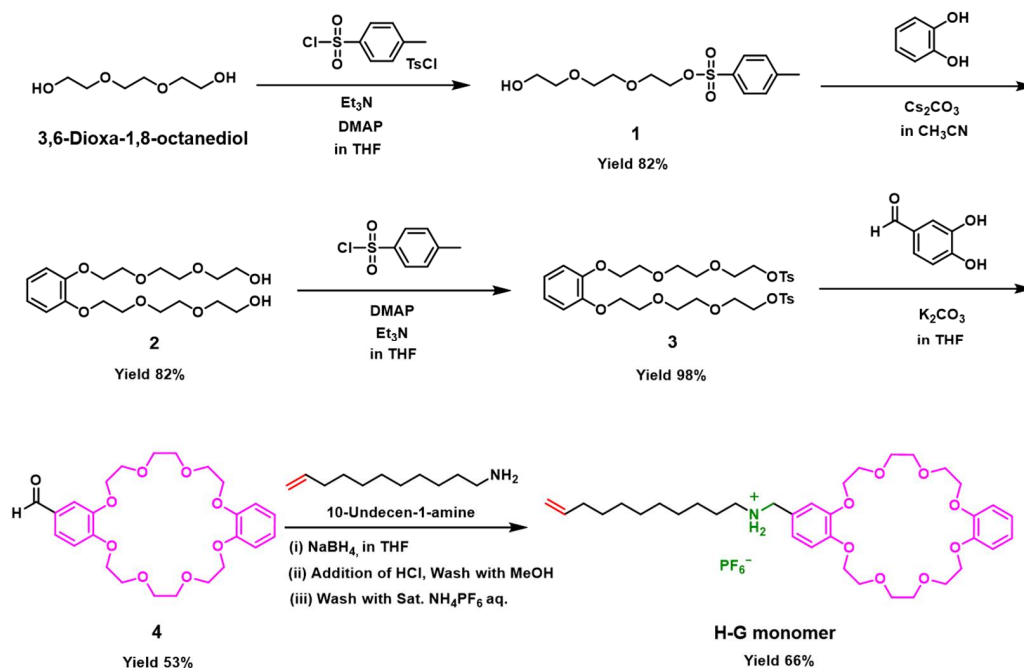
The key point of our synthetic strategy is the synthesis of a rotaxane polymer using a simple and non-dissociating inclusion structure with only a single compound. In this strategy, the bulky [c2]daisy-chain rotaxane itself acts as a stopper (pseudo-stopper), sup-

pressing the dissociation of another neighboring [c2]daisy-chain rotaxane unit. In other words, the [c2]daisy-chain rotaxane plays a dual role, as an inclusion complex and a stopper, enabling the one-pot synthesis of topological polymers with a single compound. In addition, we report the results of conducting thiol-ene reactions using dithiols to investigate the influence of distance extension between [c2]daisy-chain rotaxane units within the polymer backbone [81–85].

2. Results and Discussion

2.1. Design of H-G Monomer and Preparation of [c2]Daisy-chain Rotaxane

In order to achieve the one-pot synthesis of a poly[c2]daisy-chain rotaxane without using a third stopper compound, an H-G monomer was synthesized according to Scheme 1.

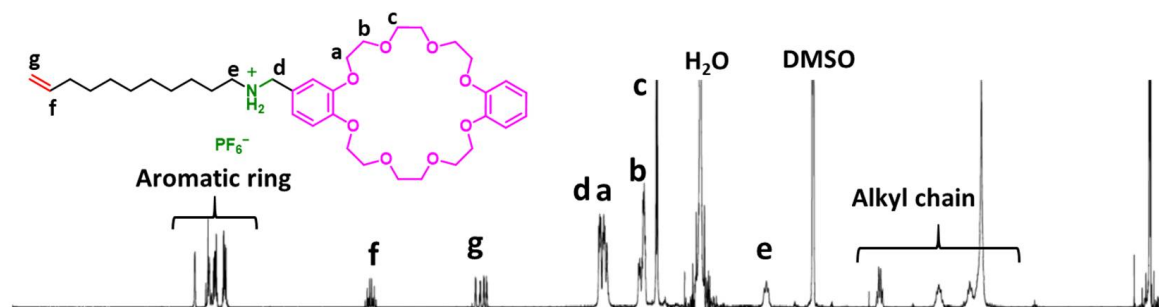
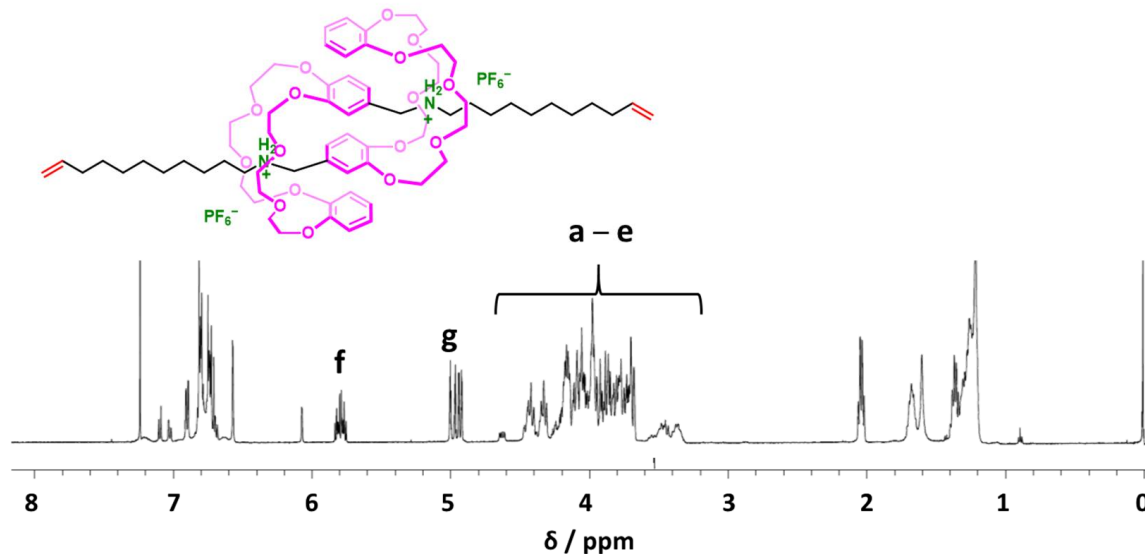


Scheme 1. Synthesis of “H-G monomer”.

There are two key features in the molecular design here. The first is the length of the alkyl chain connecting the DB24C8 and ammonium salt units. To efficiently form the [c2]daisy-chain structure between the two molecules, it is most preferable to have a length of a methylene ($-\text{CH}_2-$) for the alkyl chain, as reported for the quantitative formation of [c2]daisy-chain rotaxanes, benefiting from both the size complementarity and the π - π interactions between the benzene rings of DB24C8 [29–33,35,36]. The second feature is the incorporation of a low-radical-polymerizable terminal alkene. Long-chain alkenes without an electron-withdrawing group introduced on the adjacent carbon of the double bond easily undergo reactions involving metal coordination due to the presence of highly electron-dense double bonds while also providing high solubility in organic solvents to the entire compound. Additionally, this molecular design can easily achieve polymerization of [c2]daisy-chain rotaxane using only one compound (H-G monomer) through metathesis reactions that enable the exchange of double bonds between molecules.

The H-G monomer was successfully synthesized from 3,4-Dioxa-1,8-octanediol, two 1,2-dihydroxybenzene derivatives, and 10-undecene-1-amine in a total of 7 steps. Its structure was identified through NMR and MS measurements.

Figure 3 shows the ^1H NMR spectra of H-G monomer in $\text{DMSO}-d_6$ and CDCl_3 . Noticeable differences were observed between the two deuterated solvents, clearly indicating the presence or absence of inclusion complexes.

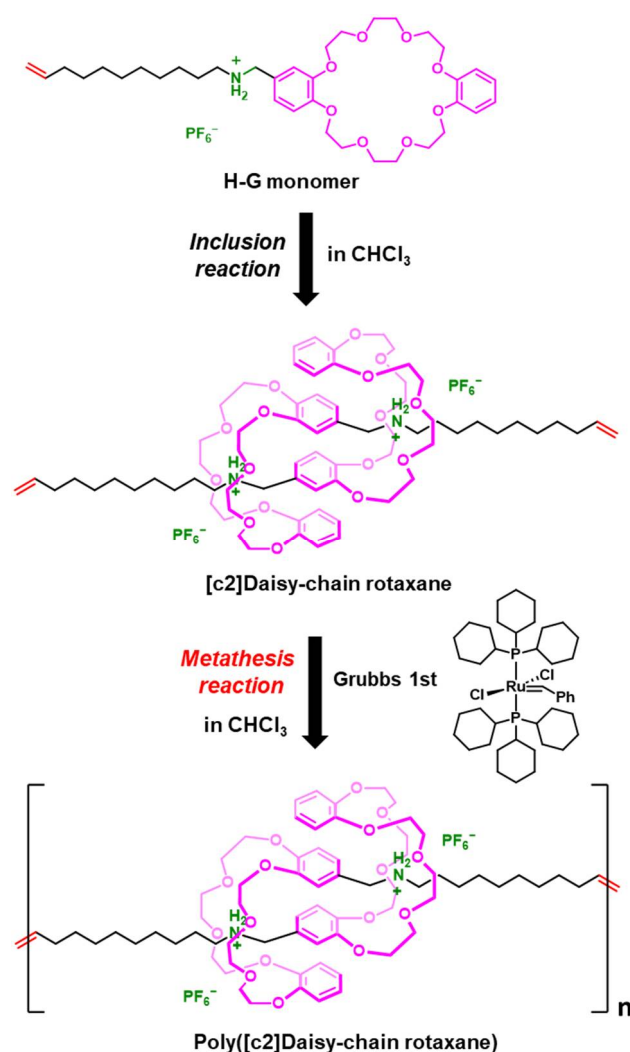
(A) H-G monomer in DMSO- d_6 (conc. 0.1 M)(B) H-G monomer in $CDCl_3$ (conc. 0.1 M)**Figure 3.** 1H NMR spectra of H-G monomer in (A) DMSO- d_6 and (B) $CDCl_3$.

In highly polar solvents such as DMSO (Figure 3A), where hydrogen bonding and electrostatic interactions between the ammonium salt and crown ether are hindered, a spectrum similar to that of the original H-G monomer was observed. Consequently, the peaks corresponding to the methylene protons a–c derived from the ethylene oxide of the crown ether, located at 4.2–3.5 ppm, and the methylene proton units d and e adjacent to the ammonium salt, became sharper and were attributed in detail.

In contrast, in the less polar solvent chloroform (Figure 3B), the assigned regions mentioned above exhibited complex splitting patterns. This is a typical peak splitting behavior observed in [c2]daisy-chain rotaxane structures, indicating the complex contribution of peak shifts and conformational changes of the DB24C8 units due to the inclusion [41]. Furthermore, even when the concentration of H-G monomer was diluted 100-fold (0.001 M), no change in the spectral shape was observed, suggesting the quantitative and stable formation of the [c2]daisy-chain rotaxane structure in chloroform (see Figure S1 in Supplementary Materials).

2.2. One-Pot Synthesis of Poly([c2]Daisy-chain Rotaxane) by Using Metathesis Reaction of H-G Monomer

Next, metathesis reactions of the H-G monomer in chloroform as a low-polarity solvent were conducted (Scheme 2). Metathesis reactions are known as powerful tools for the rearrangement of double bonds and are widely used in various molecular designs.



Scheme 2. One-pot synthesis of poly([c2]daisy-chain rotaxane) by using metathesis reaction.

In this reaction, the simultaneous formation of inclusion complexes and their polymerization allows for the synthesis of stable rotaxane materials consisting of the wheel and axle components. However, a small amount of products that do not dissolve in chloroform or other organic solvents was also present. The ^1H NMR spectrum of the chloroform-soluble part obtained through metathesis reactions is shown in Figure 4. The spectrum of the product in CDCl_3 (Figure 4A) exhibited complex splitting peaks at 4.2–3.5 ppm, similar to those of the spectrum of the [c2]daisy-chain rotaxane before the reaction (Figure 3A). Furthermore, a significant decrease in the proton peaks f and g derived from terminal double bonds at 5.8 and 5.2 ppm, respectively, and the appearance of a new proton peak h attributed to an internal double bond were observed. These observations suggest that the metathesis reaction of H-G monomer was carried out while maintaining the [c2]daisy-chain rotaxane structure. In the spectrum of the products in $\text{DMSO-}d_6$ (Figure 4B), the complex peak splitting observed in CDCl_3 changed to three distinct peaks a–c. This indicates a conformational change in the [c2]daisy-chain rotaxane, where the polar solvent DMSO strongly solvates the secondary ammonium salt unit in the rotaxane, causing the wheels to adopt a conformation that expands their distance to avoid steric hindrance without dissociating the rotaxane.

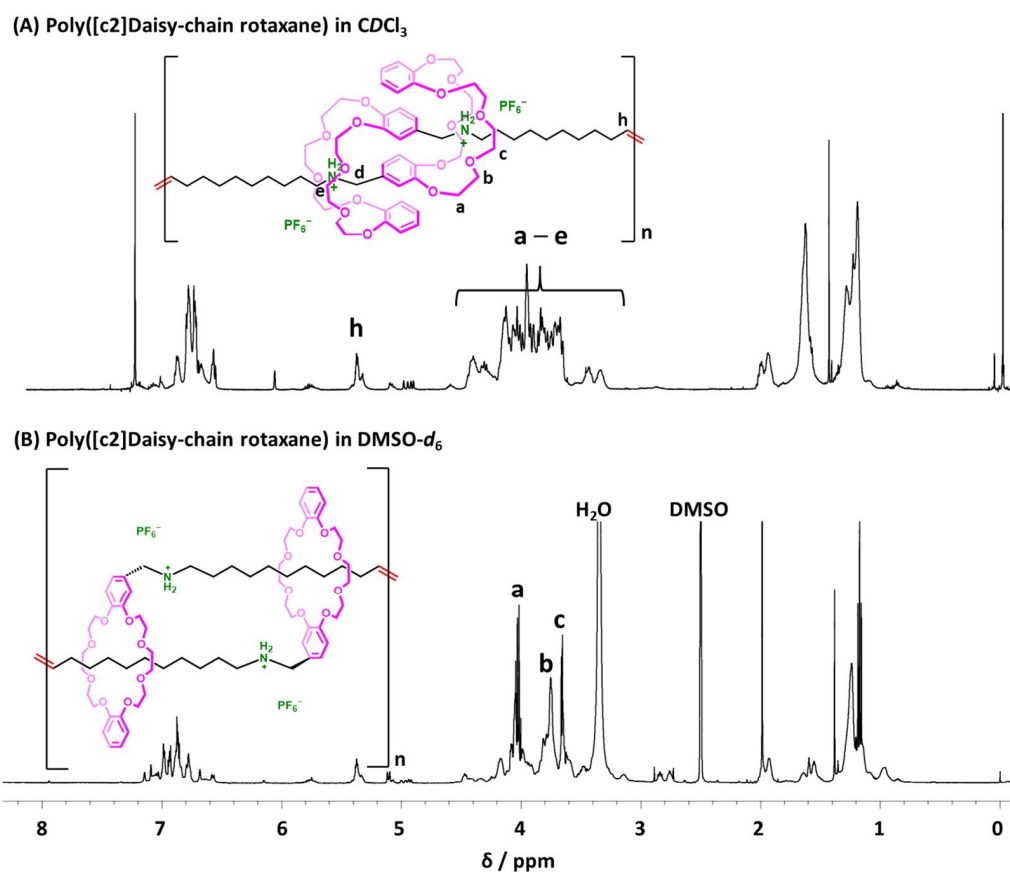


Figure 4. 1H NMR spectra of poly([c2]daisy-chain rotaxane) in (A) $CDCl_3$ and (B) $DMSO-d_6$.

The molecular weight of the obtained products was estimated using GPC measurements (Figure 5). As a result, a trimodal peak was observed at significantly different retention times from that of H-G monomer ($M_n = 670$). The average molecular weights of the trimodal peak were determined to be $M_n = 4700$ and $M_w = 5730$, with the highest molecular weight region (the filled peak area) calculated as max. $M_n = 8020$ and max. $M_w = 8830$. This indicates that the resulting products were polymers of different lengths with multiple connected [c2]daisy-chain rotaxane units, and these polymers exist stably without dissociation.

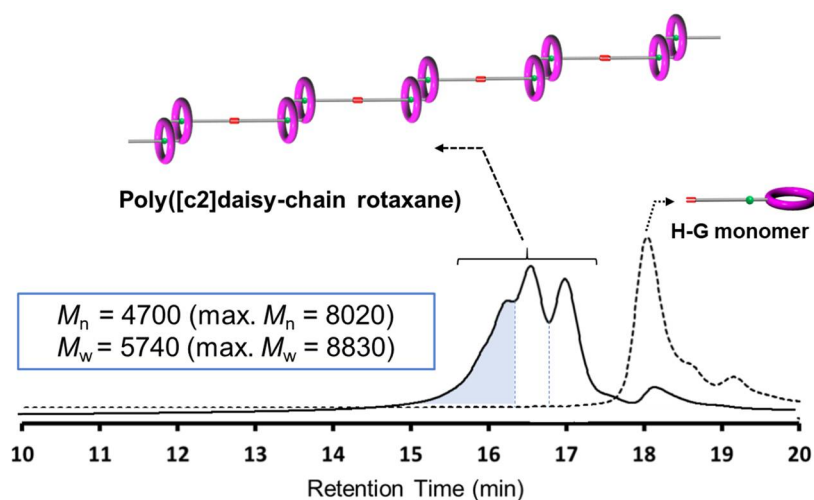
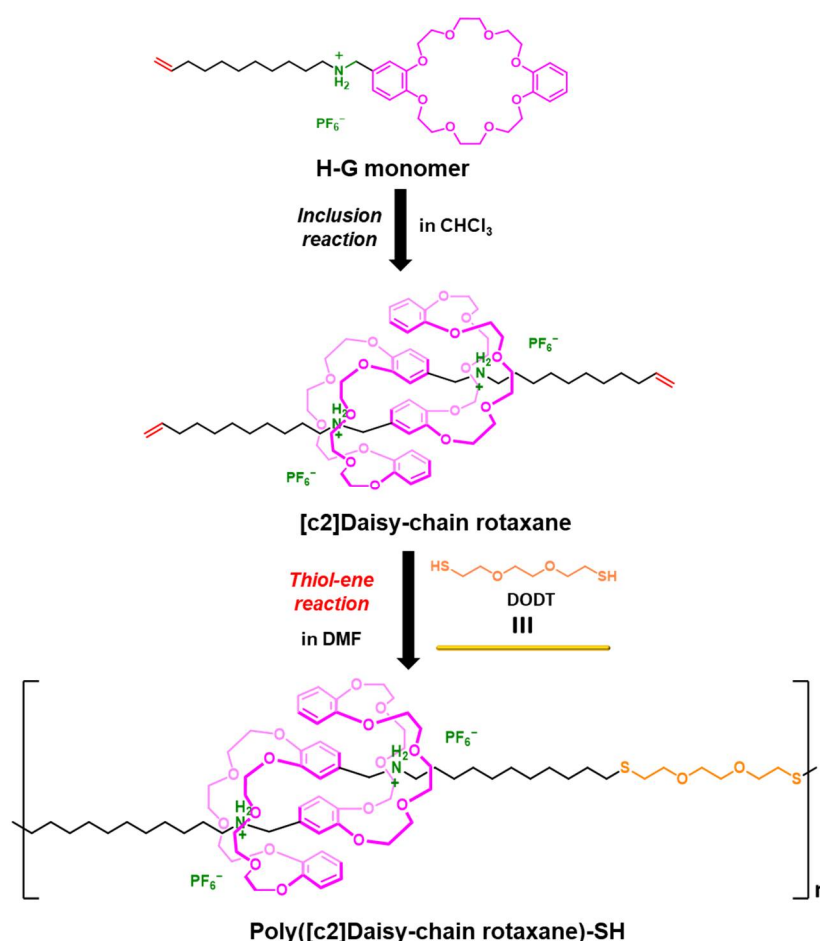


Figure 5. GPC chart of poly([c2]daisy-chain rotaxane) (eluent: $CHCl_3$).

These results demonstrate that in the metathesis reaction of H-G monomer using chloroform as the reaction solvent, both the inclusion and the polymerization reactions occur simultaneously, resulting in the formation of a high-molecular-weight polymer. In this process, adjacent [c2]daisy-chain rotaxane units act as bulky stoppers, affording the polymer to be maintained without dissociation.

2.3. One-Pot Synthesis of Poly([c2]Daisy-chain Rotaxane) by Using Thiol-Ene Reaction of H-G Monomer

In the polymerization of [c2]daisy-chain rotaxane through metathesis reaction, the obtained product showed low solubility in chloroform and a small amount of insoluble material was observed, indicating the high crystallinity of the polymer. Therefore, we investigated the change in molecular weight when introducing 3,6-dioxa-1,8-dithiol (DODT), a low-crystalline dithiol molecule, as a spacer component between [c2]daisy-chain rotaxane units (Scheme 3). H-G monomer, DODT, and benzophenone were dissolved in chloroform, and upon UV irradiation, a light-yellow solid product, poly([c2]daisy-chain rotaxane)-SH, was obtained.



Scheme 3. One-pot synthesis of poly([c2]daisy-chain rotaxane)-SH by using thiol-ene reaction.

The ¹H NMR spectrum of poly([c2]daisy-chain rotaxane)-SH exhibited a significant decrease in the proton peaks f and g originating from double bonds, as well as the same complex splitting peaks observed in poly([c2]daisy-chain rotaxane), suggesting the progression of the thiol-ene reaction during the formation of the inclusion complex (Figure 6).

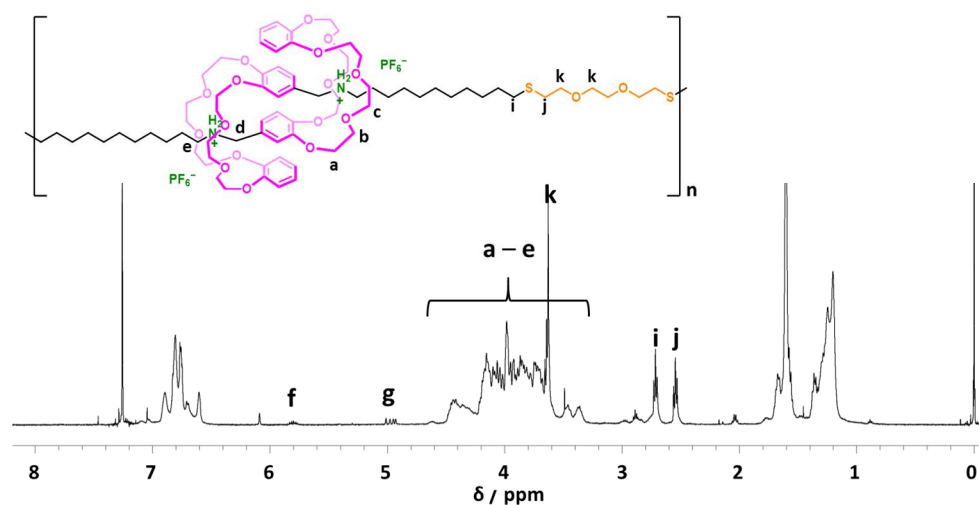


Figure 6. ^1H NMR spectrum of poly([c2]daisy-chain rotaxane)-SH in CDCl_3 .

Figure 7 shows the GPC chart of the obtained product. The chart displayed a trimodal peak, and the overall average molecular weight was $M_n = 4700$, $M_w = 5730$. Furthermore, the peak corresponding to the high-molecular-weight region (the filled peak area) was calculated as max. $M_n = 11,680$, max. $M_w = 16,660$.

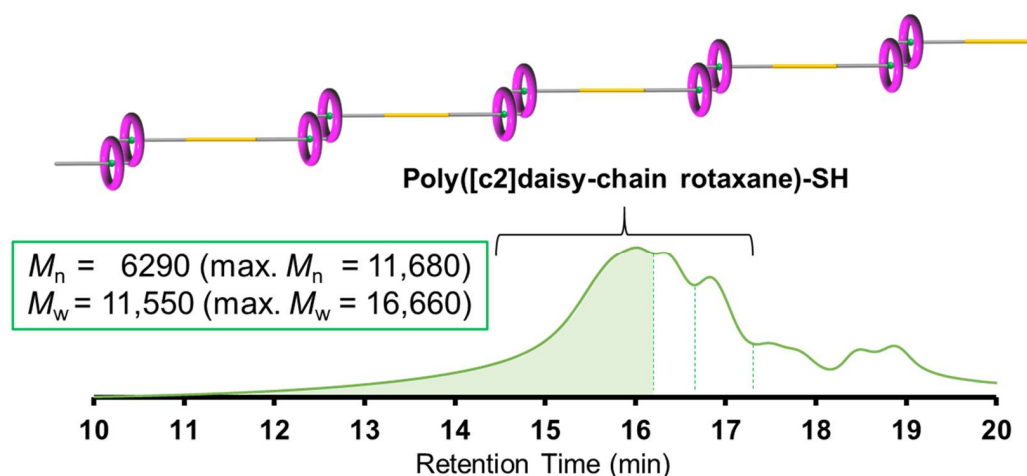
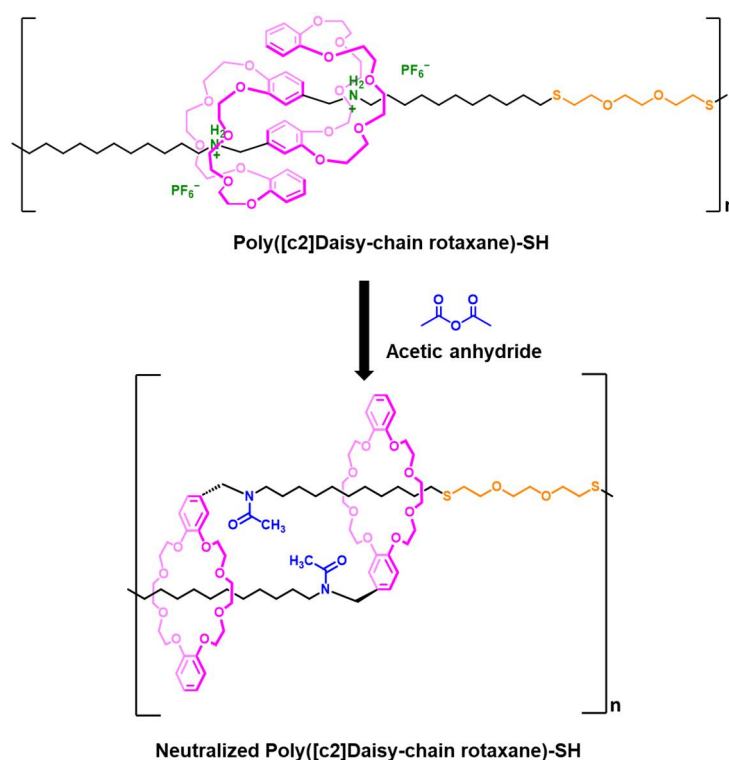


Figure 7. GPC chart of poly([c2]daisy-chain rotaxane) (eluent: CHCl_3).

These results indicate that the thiol-ene reaction system can achieve both the formation of [c2]daisy-chain rotaxane and the suppression of dissociation through the connection of rotaxanes mediated by the dithiol, resulting in a molecular weight approximately 1.5 times higher than that obtained via a metathesis reaction. This suggests that the introduction of liquid DODT components into the polymer backbone decreases the overall crystallinity and improves solubility in organic solvents. Additionally, the DSC measurement of poly([c2]daisy-chain rotaxane)-SH determined a glass transition temperature (T_g) of $43\text{ }^\circ\text{C}$, while no corresponding endothermic peak was observed in the temperature range of $20\text{--}100\text{ }^\circ\text{C}$ for the polymer obtained via a metathesis reaction (see Figure S2 in Supplementary Materials).

As the final experiment of this report, we carried out a deionization (neutralization) reaction of the highly soluble poly([c2]daisy-chain rotaxane)-SH (Scheme 4). The purpose of the neutralization reaction was to chemically remove the interaction between the ammonium salt and the crown ether that affects the [c2]daisy-chain rotaxane structure. We intentionally created an environment where the [c2]daisy-chain rotaxane could not be maintained and examined whether the polymer would disassembly.



Scheme 4. Neutralization of poly([c2]daisy-chain rotaxane)-SH with acetic anhydride.

The neutralization reaction was performed using acetic anhydride, and through IR measurements, typical absorption peaks related to the decrease in PF_6^- anions and the appearance of amide bonds confirmed the partial progression of the neutralization reaction (see Figure S3 in Supplementary Materials). In the ^1H NMR spectrum of the neutralized poly([c2]daisy-chain rotaxane)-SH, three distinct peaks a–c attributed to the crown ether were observed in the range of 4.2 to 3.6 ppm in CDCl_3 (Figure 8).

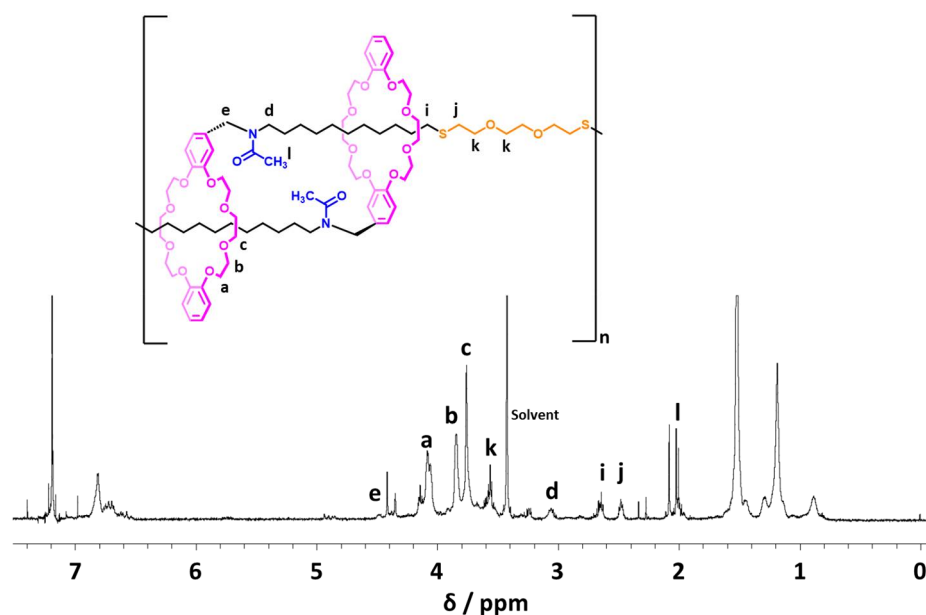


Figure 8. ^1H NMR spectrum of neutralized poly([c2]daisy-chain rotaxane)-SH in CDCl_3 .

This showed a similar chemical shift as the inclusion part in DMSO in Figure 3B, suggesting a topological change in [c2]daisy-chain rotaxane. Furthermore, the GPC measure-

ment of the obtained product showed that the average molecular weight was comparable to the molecular weight before neutralization, as $M_n = 4970$ (see Figure S4 in Supplementary Materials). In addition, the glass transition temperature of the neutralized polymer reached 3 °C, causing a further decrease in crystallinity compared to before neutralization (see Figure S5 in Supplementary Materials). This decrease suggested the involvement of the removal of interactions occurring between the secondary ammonium salt and crown ether within the [c2]daisy-chain rotaxane units. These results strongly demonstrated that the [c2]daisy-chain rotaxane significantly contributes to the structural stabilization of the polymer as a stopper.

3. Conclusions

In summary, we designed an H-G monomer in which a dibenzo-24-crown-8-ether unit and a secondary ammonium salt unit were introduced within the same molecule. We successfully achieved the one-pot synthesis of a topological polymer that remains stable without dissociation by utilizing the [c2]daisy-chain rotaxane structure. These one-pot syntheses involved the utilization of a metathesis reaction and a thiol-ene reaction. The former provided a stable polymer consisting of interconnected [c2]daisy-chain rotaxanes using only a single molecule (H-G monomer). Furthermore, the latter suggested the easy control of the solubility and crystallinity of the resulting polymer by introducing dithiol units between [c2]daisy-chain rotaxanes. Moreover, even in environments where the rotaxane structure cannot be maintained, such as polar solvents like DMSO or during neutralization processes, the resulting polymer maintained its inclusion structure without dissociation. This suggests that even when the interaction between the ammonium salt and crown ether is inhibited, the adjacent neutralized [c2]daisy-chain rotaxane functions well as a stopper and prevents the complete dissociation of their inclusion polymers. By employing this synthetic strategy, it becomes possible to conveniently synthesize various functional materials with [c2]daisy-chain rotaxane structures, contributing to a wide range of fields such as stretchable materials, stimuli-responsive materials, and self-healing materials. Currently, our focus is on material design tailored to specific applications, and we are proceeding with synthesis and evaluation.

4. Experimental Section

4.1. Materials and Instruments

Reagent-grade solvents (hexane, dichloromethane, chloroform, tetrahydrofuran (THF), acetone, methanol (MeOH), ethyl acetate (EtOAc), and dimethylformamide (DMF)) and other chemicals were used without further purification. Thin-layer chromatography was performed using MERCK (Darmstadt, Germany) 60 F₂₅₄, and MERCK 60 (0.063–0.200 mm) was used as silica gel.

¹H NMR (500 MHz) and ¹³C NMR (270 MHz) spectra were recorded on a JEOL JNM-ECA500 instrument using CDCl₃ or DMSO-*d*₆ as the deuterated solvent and tetramethyl silane (TMS) as the internal standard. Molecular weights and molecular weight distributions were estimated via gel permeation chromatography (GPC) experiments conducted on a SHIMADZU SPD-20A instrument equipped with an ultraviolet (UV) detector (257 nm) and a Shodex GPC KF-804L column (internal diameter, 8.0 mm; length, 30 cm; gel particle diameter, 7 μm; theoretical plate number >18,000). Tetrahydrofuran (CDCl₃) was used as an eluent at a flow rate of 1.0 mL/min. Molecular weights were calibrated against polystyrene standards. Accurate mass measurements with electrospray ionization time-of-flight (ESI-TOF) mass were performed using a Waters Xevo(TM) G2-XS QToF. Fourier-transform infrared (FT-IR) spectra were recorded using a JASCO FTIR-6600, as well as a spectrometer. The glass transition temperature was measured using a highly sensitive differential scanning calorimeter Hitachi High-Tech Science DSC 7020.

4.2. Synthesis of Compound 1

A THF solution (200 mL) containing 3,4-Dioxa-1,8-octanediol (90.2 g, 0.599 mol), triethylamine (12.1 g, 0.120 mol), and 4-dimethylaminopyridine (DMAP) (0.146 g, 1.20 mmol) was slowly added dropwise to a THF solution (100 mL) of *p*-toluenesulfonic chloride (TsCl) (45.8 g, 0.240 mol). The resulting mixture was stirred at room temperature for 24 h. Subsequently, the solution was treated with saturated sodium bicarbonate solution (50 mL) and then diluted with EtOAc (300 mL). It was washed three times with water (100 mL). The organic layer obtained was dried over anhydrous magnesium sulfate and concentrated under reduced pressure. The residue was purified via column chromatography using silica gel and an eluent of EtOAc. Compound 1, a colorless and transparent oil, was obtained (9.36 g, 81.9% yield). ¹H NMR (500 MHz, CDCl₃) δ (ppm from TMS): 7.91–7.89 (d, 2H, Ph), 7.39–7.33 (d, 2H, Ph), 4.20–4.17 (t, 2H, Ts–OCH₂–), 3.80–3.58 (m, 10H, Ts–OCH₂CH₂–OCH₂CH₂–OCH₂CH₂–OH), 2.42 (s, 3H, CH₃–Ph) (see Figure S6 in Supplementary Materials) [86].

4.3. Synthesis of Compound 2

Pyrocatechol (1.35 g, 0.0123 mol) was added to a suspension of cesium carbonate (8.01 g, 0.0246 mol) in acetonitrile (100 mL) and refluxed for 1 h. Then, the acetonitrile solution (50 mL) containing compound 1 (9.36 g, 0.0307 mol) was slowly added dropwise and refluxed for 24 h. After cooling to 25 °C, the suspension was filtered, and the filtrate was concentrated under reduced pressure. The residue was purified via column chromatography using silica gel and an eluent of EtOAc/MeOH (4/1, *v/v*). Compound 2, a yellow viscous oil, was obtained (9.43 g, 82.4% yield). ¹H NMR (500 MHz, CDCl₃) δ (ppm from TMS): 6.92 (s, 4H, Ph), 4.20–4.15 (t, 4H, Ph–OCH₂–), 3.88–3.60 (m, 20H, Ph–OCH₂CH₂–OCH₂CH₂–OCH₂CH₂–OH) (see Figure S7 in Supplementary Materials) [87].

4.4. Synthesis of Compound 3

A THF solution (30 mL) containing compound 2 (5.88 g, 0.0175 mol), triethylamine (7.08 g, 0.0471 mol), and DMAP (0.0405 g, 0.314 mmol) was slowly added dropwise to a THF solution (20 mL) of TsCl (8.97 g, 0.0471 mol), and the mixture was stirred at 25 °C for 12 h. Then, the solution was treated with saturated sodium bicarbonate solution (50 mL) and diluted with ethyl acetate (200 mL), followed by three washes with water (100 mL). The organic layer obtained was dried over anhydrous magnesium sulfate and concentrated under reduced pressure. The residue was purified via column chromatography using silica gel and an eluent of ethyl acetate/hexane (2/1, *v/v*). Compound 3, a yellow viscous oil, was obtained (5.76 g, 97.9% yield). ¹H NMR (500 MHz, CDCl₃) δ (ppm from TMS): 7.80–7.75 (d, 4H, Ph (Ts)), 7.38–7.29 (d, 4H, Ph (Ts)), 6.90 (s, 4H, Ph), 4.18–4.11 (t, 4H, Ph–OCH₂–), 3.88–3.59 (m, 20H, Ph–OCH₂CH₂–OCH₂CH₂–OCH₂CH₂–OH), 2.44 (s, 6H, CH₃–Ph) (see Figure S8 in Supplementary Materials) [87].

4.5. Synthesis of Compound 4

Compound 3 was added to a THF suspension (300 mL) of potassium carbonate (8.15 g, 25.4 mmol) and refluxed for one hour. Then, a THF solution (100 mL) of 3,4-dihydroxybenzaldehyde (0.696 g, 5.45 mmol) was added dropwise to the solution, and the mixture was refluxed for 24 h. After quenching with 1 M HCl aqueous solution, the mixture was diluted with dichloromethane (200 mL) and washed with saturated sodium chloride solution (100 mL). The organic layer was dried over anhydrous magnesium sulfate and concentrated under reduced pressure. The resulting concentrate was purified via column chromatography using silica gel and an eluent of ethyl acetate/methanol (10/1, *v/v*). Mono-formylated DB24C8 (compound 4), a white solid, was obtained (1.77 g, 52.9% yield). ¹H NMR (500 MHz, CDCl₃) δ (ppm from TMS): 9.83–9.81 (s, 1H, Ph–CHO), 7.81–7.75 (m, 5H, Ph), 7.35–7.29 (d, 2H, Ph), 4.23–4.08 (m, 24H, –CH₂CH₂O–) (see Figure S8 in Supplementary Materials) [87].

4.6. Synthesis of Compound 5

A THF solution (10 mL) of compound 4 was slowly added dropwise to a THF solution (10 mL) of 10-undecen-1-amine (0.720 g, 4.25 mmol), and the resulting mixture was stirred at 25 °C for 8 h. The solvent was removed under reduced pressure, yielding compound 5 with reduced formyl groups as a yellow solid (crude product, 1.31 g). It was used without further purification in the subsequent reaction. ¹H NMR (500 MHz, CDCl₃, crude sample) δ (ppm from TMS): 8.11–8.09 (s, 1H, Ph–CH=N), 6.88–6.80 (m, 7H, Ph), 5.82–5.73 (m, 2H, CH₂=CH–), 4.98–4.87 (m, 1H, CH₂=CH–), 4.21–3.78 (m, 24H, –CH₂CH₂O–), 3.61–3.50 (m, 2H, CH=N–CH₂–), 2.03–1.90 (m, 2H, CH₂=CH–CH₂–), 1.73–1.67 (m, 2H, =N–CH₂–CH₂–), 1.37–1.20 (m, 12H, CH₂=CH–(CH₂)₆–) (see Figure S9 in Supplementary Materials).

4.7. Synthesis of H-G Monomer

Compound 5 (1.80 g, 2.86 mmol) was dissolved in methanol (2 mL), and 1 M HCl aqueous solution (2 mL) was added dropwise. The resulting mixture was stirred at 25 °C for 1 h. MeOH was removed under reduced pressure, and the residue was diluted with dichloromethane (20 mL). The solution was washed with saturated NH₄PF₆ aqueous solution (10 mL × 2 times). The organic layer was concentrated under reduced pressure, and the obtained residue was washed with ethyl acetate, resulting in the white solid H-G monomer (1.00 g, 66% yield). ¹H NMR (500 MHz, DMSO-*d*₆) δ (ppm from TMS): 7.02–6.84 (m, 7H, Ph), 5.83–5.74 (m, 1H, CH₂=CH–), 5.02–4.91 (m, 2H, CH₂=CH–), 4.10–4.01 (m, 10H, –Ph–CH₂–NH₂⁺–, –PhO–CH₂CH₂O–), 3.81–3.75 (m, 8H, –PhO–CH₂CH₂O–), 3.66–3.63 (m, 8H, –PhO–CH₂CH₂O–CH₂CH₂O–), 2.87–2.82 (m, –Ph–CH₂–NH₂⁺–CH₂–), 2.04–1.99 (m, 2H, CH₂=CH–CH₂–), 1.38–1.20 (m, 14H, CH₂=CH–CH₂–(CH₂)₆–). ¹³C NMR (270 MHz, DMSO-*d*₆) δ (ppm from TMS): 148.96, 139.34, 125.06, 123.44, 121.69, 115.22, 70.97, 69.21, 50.36, 46.77, 40.06, 33.77, 29.06, 26.52, 19.15, 29.07 (see Figure S10 in Supplementary Materials). ESI-TOF-MS: *m/z* calculated for C₇₂H₁₁₀N₂O₁₆Na [M + Na]⁺ 652.3827; found.

4.8. Synthesis of Poly([c2]Daisy-chain Rotaxane)

To a solution of H-G monomer (0.306 g, 0.193 mmol) in chloroform (15 mL), benzyldienebis(tricyclohexylphosphine)dichlororuthenium (Grubbs 1st, 1.00 mg, 1.22 nmol) was added; the mixed solution was stirred at 50 °C for 24 h, and then the solvent was removed under reduced pressure, followed by washing with MeOH to give a light purple solid product (0.300 g, crude product). ¹H NMR (500 MHz, CDCl₃, CHCl₃-soluble part) δ (ppm from TMS): 6.98–6.55 (m, 14H, Ph), 5.41–5.35 (m, 2H, CH₂=CH–), 4.50–4.21 (m, 4H, –Ph–CH₂–NH₂⁺–), 4.21–3.63 (m, 48H, –CH₂CH₂O–), 3.50–3.30 (m, 4H, –Ph–CH₂–NH₂⁺–CH₂–), 2.06–1.99 (m, 4H, CH₂=CH–CH₂–), 1.40–1.16 (m, 28H, CH₂=CH–CH₂–(CH₂)₇–).

4.9. Synthesis of Poly([c2]Daisy-chain Rotaxane)-SH

A solution of H-G monomer (0.300 g, 0.193 mmol), 3,6-dioxa-1,8-dithiol (Dithiol) (0.0364 g, 0.199 mmol), and benzophenone (0.0035 g, 0.0193 mmol) in acetonitrile (2 mL) was subjected to UV irradiation, and the resulting mixture was reprecipitated with methanol to obtain a light-yellow solid product (0.313 g yield, crude product). ¹H NMR (500 MHz, CDCl₃) δ (ppm from TMS): 6.90–6.60 (m, 14H, Ph), 4.50–4.20 (d, 4H, Ph–CH₂–NH₂⁺–), 4.20–3.65 (m, 52H, –CH₂CH₂O–, –S–CH₂–CH₂–), 3.65–3.58 (d, 8H, S–CH₂–CH₂–O–CH₂–CH₂–O, CH₂–CH₂–S–), 3.53–3.29 (d, 4H, –Ph–CH₂–NH₂⁺–CH₂–), 2.76–2.68 (m, 2H, –(CH₂)₁₀–CH₂–S–), 2.58–2.36 (m, 4H, –O–CH₂–CH₂–S–), 1.98–1.51 (m, 2H, –O–CH₂–CH₂–S–CH₂–CH₂–), 1.40–1.15 (m, 36H, –(CH₂)₉–).

4.10. Synthesis of Neutralized Poly([c2]Daisy-chain Rotaxane)-SH

Poly([c2]daisy-chain rotaxane) 2 (0.107 g, 68.8 nmol) was dissolved in DMF (1 mL), and acetic anhydride (1.30 g, 12.7 mmol) was added. The mixture was stirred at 90 °C for 24 h. The resulting product was obtained as a reddish-brown oil through reprecipitation using methanol (0.0460 g yield, crude product). ¹H NMR (500 MHz, CDCl₃) δ (ppm from TMS): 6.90–6.55 (m, 14H, Ph), 4.50–4.30 (m, 4H, Ph–CH₂–N(OCH₃)–), 4.20–4.10 (m, 8H, Ph–

O-CH₂-CH₂-O-CH₂-), 3.90–3.70 (d, 16H, Ph-O-CH₂-CH₂-O-CH₂-), 3.65–3.50 (m, 8H, -CH₂-S-CH₂-CH₂-O-CH₂-CH₂-O-, CH₂-CH₂-S-), 3.18–3.01 (s, 4H, Ph-CH₂-N(OCH₃)-CH₂-), 2.76–2.68 (m, 4H, -(CH₂)₁₀-CH₂-S-), 2.58–2.36 (m, 4H, -O-CH₂-CH₂-S-), 2.03–1.98 (m, 6H, Ph-CH₂-N(OCH₃)-), 1.50–1.10 (m, 36H, -(CH₂)₁₀-).

Supplementary Materials: The following supporting information can be downloaded at: <https://www.mdpi.com/article/10.3390/reactions4030027/s1>, Figure S1: ¹H NMR spectra of H-G monomer at (A) conc. 0.1 M, (B) 0.01, and (C) 0.001 M in CDCl₃; Figure S2: DSC charts of poly([c2]daisy-chain rotaxane) and poly([c2]daisy-chain rotaxane)-SH; Figure S3: IR spectra of poly([c2]daisy-chain rotaxane)-SH and neutralized poly([c2]daisy-chain rotaxane)-SH; Figure S4: GPC chart of neutralized poly([c2]Daisy-chain rotaxane (eluent: CHCl₃); Figure S5: DSC charts of neutralized poly([c2]Daisy-chain rotaxane); Figures S6–S9: ¹H NMR spectra of compound 1–4 in CDCl₃; Figure S10: ¹³C NMR spectra of H-G monomer in CDCl₃.

Author Contributions: Conceptualization, R.K., K.O. and K.Y.; synthesis and structural analysis, R.K.; writing—original draft preparation, K.Y. All authors have read and agreed to the published version of the manuscript.

Funding: This research received no external funding.

Data Availability Statement: The data presented in this study are available upon request from the corresponding author. The data are not publicly available because of the lack of a dedicated server.

Conflicts of Interest: The authors declare no conflict of interest.

References

1. Harada, A.; Kamachi, M. Complex formation between cyclodextrin and poly(propylene glycol). *J. Chem. Soc. Chem. Commun.* **1990**, *19*, 1322–1323. [[CrossRef](#)]
2. Harada, A.; Li, J.; Kamachi, M. The molecular necklace: A rotaxane containing many threaded α -cyclodextrins. *Nature* **1992**, *356*, 325–327. [[CrossRef](#)]
3. Harada, A.; Li, J.; Kamachi, M. Synthesis of a tubular polymer from threaded cyclodextrins. *Nature* **1993**, *364*, 516–518. [[CrossRef](#)]
4. Harada, A.; Li, J.; Nakamitsu, T.; Kamachi, M. Preparation and characterization of polyrotaxanes containing many threaded α -cyclodextrins. *J. Org. Chem.* **1993**, *58*, 7524–7528. [[CrossRef](#)]
5. Harada, A.; Li, J.; Kamachi, M. Preparation and Characterization of a Polyrotaxane Consisting of Monodisperse Poly(ethylene glycol) and α -Cyclodextrins. *J. Am. Chem. Soc.* **1994**, *116*, 3192–3196. [[CrossRef](#)]
6. Harada, A.; Li, J.; Kamachi, M. Double-stranded inclusion complexes of cyclodextrin threaded on poly(ethylene glycol). *Nature* **1994**, *370*, 126–128. [[CrossRef](#)]
7. Harada, A. Design and construction of supramolecular architectures consisting of cyclodextrins and polymers. *Adv. Polym. Sci.* **1997**, *133*, 141–191. [[CrossRef](#)]
8. Harada, A.; Li, J.; Kamachi, M. Molecular recognition: Preparation of polyrotaxane and tubular polymer from cyclodextrin. *Polym. Adv. Technol.* **1997**, *8*, 241–249. [[CrossRef](#)]
9. Harada, A.; Li, J.; Kamachi, M. Non-ionic [2]rotaxanes containing methylated α -cyclodextrins. *Chem. Commun.* **1997**, *15*, 1413–1414. [[CrossRef](#)]
10. Harada, A. Construction of supramolecular structures from cyclodextrins and polymers. *Carbohydr. Polym.* **1997**, *34*, 183–188. [[CrossRef](#)]
11. Okada, M.; Kamachi, M.; Harada, A. Preparation and Characterization of Inclusion Complexes between Methylated Cyclodextrins and Poly(tetrahydrofuran). *Macromolecules* **1999**, *32*, 7202–7207. [[CrossRef](#)]
12. Ashton, P.R.; Grogan, M.; Slawin, A.M.Z.; Stoddart, J.F.; Williams, D.J. The template-directed synthesis of a [2]rotaxane. *Tetrahedron Lett.* **1991**, *32*, 6235–6238. [[CrossRef](#)]
13. Ashton, P.R.; Philp, D.; Spencer, N.; Stoddart, J.F. The self-assembly of [n]pseudorotaxanes. *J. Chem. Soc.* **1991**, *23*, 1677–1679. [[CrossRef](#)]
14. Shen, Y.X.; Gibson, H.W. Synthesis and some properties of polyrotaxanes comprised of polyurethane backbone and crown ethers. *Macromolecules* **1992**, *25*, 2058–2059. [[CrossRef](#)]
15. Ashton, P.R.; Philp, D.; Spencer, N.; Stoddart, J.F. A new design strategy for the self-assembly of molecular shuttles. *J. Chem. Soc.* **1992**, *16*, 1124–1128. [[CrossRef](#)]
16. Gibson, H.W.; Marand, H. Polyrotaxanes: Molecular composites derived by physical linkage of cyclic and linear species. *Adv. Mater.* **1993**, *5*, 11–21. [[CrossRef](#)]
17. Bissell, R.A.; Cordova, E.; Kaifer, A.E.; Stoddart, J.F. A chemically and electrochemically switchable molecular shuttle. *Nature* **1994**, *369*, 133–137. [[CrossRef](#)]

18. Diederich, F.; Dietrich-Buchecker, C.; Nierengarten, J.; Sauvage, J.P. A copper(I)-complexed rotaxane with two fullerene stoppers. *J. Chem. Soc.* **1995**, *7*, 781–782. [[CrossRef](#)]
19. Gibson, H.W.; Liu, S.; Lecavalier, P.; Wu, C.; Shen, Y.X. Synthesis and Preliminary Characterization of Some Polyester Rotaxanes. *J. Am. Chem. Soc.* **1995**, *117*, 852–874. [[CrossRef](#)]
20. Ashton, P.R.; Glink, P.T.; Martinez-Diaz, M.; Stoddart, J.F.; White, A.J.P.; Williams, D.J. Thermodynamically controlled self-assembly of pseudorotaxanes and pseudopolyrotaxanes with different recognition motifs operating self-selectively. *Angew. Chem. Int. Ed.* **1996**, *35*, 1930–1933. [[CrossRef](#)]
21. Gong, C.; Gibson, H.W. Synthesis and Characterization of a Polyester/Crown Ether Rotaxane Derived from a Difunctional Blocking Group. *Macromolecules* **1996**, *29*, 7029–7033. [[CrossRef](#)]
22. Cao, J.; Fyfe, M.C.T.; Stoddart, J.F.; Cousins, G.R.L.; Glink, P.T. Molecular Shuttles by the Protecting Group Approach. *J. Chem. Soc.* **2000**, *65*, 1937–1946. [[CrossRef](#)] [[PubMed](#)]
23. Kraus, T.; Budesinsky, M.; Cvacka, J.; Sauvage, J.P. Copper(I)-directed formation of a cyclic pseudorotaxane tetramer and its trimeric homologue. *Angew. Chem. Int. Ed.* **2006**, *45*, 258–261. [[CrossRef](#)] [[PubMed](#)]
24. Nakazono, K.; Kuwata, S.; Takata, T. Crown ether–tert-ammonium salt complex fixed as rotaxane and its derivation to nonionic rotaxane. *Tetrahedron Lett.* **2008**, *49*, 2397–2401. [[CrossRef](#)]
25. Zhu, N.; Nakazono, K.; Takata, T. Solid-state Rotaxane Switch: Synthesis of Thermoresponsive Rotaxane Shuttle Utilizing a Thermally Decomposable Acid. *Chem. Lett.* **2016**, *45*, 445–447. [[CrossRef](#)]
26. Takata, T.; Kawasaki, H.; Asai, S.; Furusho, Y.; Kihar, N. Conjugate addition-approach to end-capping of pseudorotaxanes for rotaxane synthesis. *Chem. Lett.* **1999**, *3*, 223–224. [[CrossRef](#)]
27. Okumura, Y.; Ito, K. The Polyrotaxane Gel: A Topological Gel by Figure-of-Eight Cross-links. *Adv. Mater.* **2001**, *13*, 485–487. [[CrossRef](#)]
28. Oku, T.; Furusho, Y.; Takata, T. A concept for recyclable cross-linked polymers: Topologically networked polyrotaxane capable of undergoing reversible assembly and disassembly. *Angew. Chem. Int. Ed.* **2004**, *43*, 966–969. [[CrossRef](#)]
29. Takata, T. Polyrotaxane and Polyrotaxane Network: Supramolecular Architectures Based on the Concept of Dynamic Covalent Bond Chemistry. *Polym. J.* **2006**, *38*, 1–20. [[CrossRef](#)]
30. Yamabuki, K.; Isobe, Y.; Onimura, K.; Oishi, T. Pseudorotaxane-coupled Gel: A New Concept of Interlocked Gel Synthesis by Using Metathesis Reaction. *Polym. J.* **2008**, *40*, 205–211. [[CrossRef](#)]
31. Zhang, Y.; Zhou, Q.; Jia, S.; Lin, K.; Fan, G.; Yuan, J.; Yu, S.; Shi, J. Specific Modification with TPGS and Drug Loading of Cyclodextrin Polyrotaxanes and the Enhanced Antitumor Activity Study In Vitro and In Vivo. *ACS Appl. Mater. Interfaces* **2019**, *11*, 46427–46436. [[CrossRef](#)] [[PubMed](#)]
32. Takata, T. Switchable Polymer Materials Controlled by Rotaxane Macromolecular Switches. *ACS Cent. Sci.* **2020**, *6*, 129–143. [[CrossRef](#)] [[PubMed](#)]
33. Uenuma, S.; Maeda, R.; Yokoyama, H.; Ito, K. Molecular Recognition of Fluorescent Probe Molecules with a Pseudopolyrotaxane Nanosheet. *ACS Macro Lett.* **2021**, *10*, 237–242. [[CrossRef](#)] [[PubMed](#)]
34. Mohammed, A.F.A.; Othman, M.H.; Taharabaru, T.; Elamin, K.M.; Ito, K.; Inoue, M.; El-Badry, M.; Saleh, K.I.; Onodera, R.; Motoyama, K. Stabilization and Movable Ligand-Modification by Folate-Appended Polyrotaxanes for Systemic Delivery of siRNA Polyplex. *ACS Macro Lett.* **2022**, *11*, 1225–1229. [[CrossRef](#)]
35. Wang, Y.; Li, Z.; Xu, H.; Wang, Q.; Peng, W.; Chi, S.; Wang, C.; Wang, J.; Deng, Y. Polymer-in-Salt Electrolyte from Poly(caprolactone)-graft-polyrotaxane for Ni-Rich Lithium Metal Batteries at Room Temperature. *ACS Appl. Mater. Interfaces* **2023**, *15*, 31552–31560. [[CrossRef](#)]
36. Mayumi, K.; Ito, K. Structure and dynamics of polyrotaxane and slide-ring materials. *Polymer* **2010**, *51*, 959–967. [[CrossRef](#)]
37. Hoshino, T.; Miyauchi, M.; Kawaguchi, Y.; Yamaguchi, H.; Harada, A. Daisy Chain Necklace: Tri[2]rotaxane Containing Cyclodextrins. *J. Am. Chem. Soc.* **2000**, *122*, 9876–9877. [[CrossRef](#)]
38. Jiménez, M.C.; Dietrich-Buchecker, C.; Sauvage, J.P. Towards Synthetic Molecular Muscles: Contraction and Stretching of a Linear Rotaxane Dimer. *Angew. Chem. Int. Ed.* **2000**, *39*, 3284–3287. [[CrossRef](#)]
39. Amirsakis, D.G.; Elizarov, A.M.; Garcia-Garibay, M.A.; Glink, P.T.; Stoddart, J.F.; White, A.J.P.; Williams, D.J. Diastereospecific Photochemical Dimerization of a Stilbene-Containing Daisy Chain Monomer in Solution as well as in the Solid State. *Angew. Chem. Int. Ed.* **2003**, *42*, 1126–1132. [[CrossRef](#)]
40. Tsukagoshi, S.; Miyawaki, A.; Takashima, Y.; Yamaguchi, Y.; Harada, A. Contraction of Supramolecular Double-Threaded Dimer Formed by α -Cyclodextrin with a Long Alkyl Chain. *Org. Lett.* **2007**, *9*, 1053–1055. [[CrossRef](#)]
41. Coutrot, F.; Romuald, C.; Busseron, E. A New pH-Switchable Dimannosyl[c2]Daisy Chain Molecular Machine. *Org. Lett.* **2008**, *10*, 3741–3744. [[CrossRef](#)] [[PubMed](#)]
42. Wu, J.; Leung, K.C.F.; Britz, D.; Han, J.Y.; Cantrill, S.J.; Fang, L.; Stoddart, J.F. An Acid–Base-Controllable [c2]Daisy Chain. *Angew. Chem. Int. Ed.* **2008**, *47*, 7470–7474. [[CrossRef](#)] [[PubMed](#)]
43. Romuald, C.; Busseron, E.; Coutrot, F. Very Contracted to Extended co-Conformations with or without Oscillations in Two- and Three-Station [c2]Daisy Chains. *J. Org. Chem.* **2010**, *75*, 6516–6531. [[CrossRef](#)] [[PubMed](#)]
44. Zheng, B.; Klautzsch, F.; Xue, M.; Huang, F.; Schalley, C.A. Self-sorting of crown ether/secondary ammonium ion hetero-[c2]daisy chain pseudorotaxanes. *Org. Chem. Front.* **2014**, *1*, 532–540. [[CrossRef](#)]
45. Bruns, C.J.; Stoddart, J.F. Rotaxane-Based Molecular Muscles. *Acc. Chem. Res.* **2014**, *47*, 2186–2199. [[CrossRef](#)]

46. Wolf, A.; Moulin, E.; Cid, J.J.; Goujon, A.; Du, G.; Busseron, E.; Fuks, G.; Giuseppone, N. pH and light-controlled self-assembly of bistable [c2] daisy chain rotaxanes. *Chem. Commun.* **2015**, *51*, 4212–4215. [[CrossRef](#)]
47. Goujon, A.; Du, G.; Moulin, E.; Fuks, G.; Maaloum, M.; Buhler, E.; Giuseppone, N. Hierarchical Self-Assembly of Supramolecular Muscle-Like Fibers. *Angew. Chem.* **2015**, *55*, 703–707. [[CrossRef](#)]
48. Fu, X.; Zhang, Q.; Rao, S.J.; Qu, D.H.; Tian, H. One-pot synthesis of a [c2]daisy-chain-containing hetero[4]rotaxane via a self-sorting strategy. *Chem. Sci.* **2016**, *7*, 1696–1701. [[CrossRef](#)]
49. Wang, P.; Gao, Z.; Yuan, M.; Zhu, J.; Wang, F. Mechanically linked poly[2]rotaxanes constructed from the benzo-21-crown-7/secondary ammonium salt recognition motif. *Polym. Chem.* **2016**, *7*, 3664–3668. [[CrossRef](#)]
50. Aoki, D.; Aibara, G.; Uchida, S.; Takata, T. A Rational Entry to Cyclic Polymers via Selective Cyclization by Self-Assembly and Topology Transformation of Linear Polymers. *J. Am. Chem. Soc.* **2017**, *139*, 6791–6794. [[CrossRef](#)]
51. Zhang, Q.; Rao, S.; Xie, T.; Li, X.; Xu, T.; Li, D.; Qu, D.; Long, Y.; Tian, H. Muscle-like Artificial Molecular Actuators for Nanoparticles. *Chem* **2018**, *4*, 2670–2684. [[CrossRef](#)]
52. Rao, S.J.; Ye, X.H.; Zhang, Q.; Gao, C.; Wang, W.Z.; Qu, D.H. Light-Induced Cyclization of A [c2]Daisy-Chain Rotaxane to Form a Shrinkable Double-Lasso Macrocycle. *Asian J. Org. Chem.* **2018**, *7*, 902–905. [[CrossRef](#)]
53. Wolf, A.; Cid, J.-J.; Moulin, E.; Niess, F.; Du, G.; Goujon, A.; Busseron, E.; Ruff, A.; Ludwigs, S.; Giuseppone, N. Unsymmetric Bistable [c2]Daisy Chain Rotaxanes which Combine Two Types of Electroactive Stoppers. *Eur. J. Org. Chem.* **2019**, *2019*, 3421–3432. [[CrossRef](#)]
54. Van Raden, J.M.; Jarenwattananon, N.N.; Zakharov, L.N.; Jasti, R. Active Metal Template Synthesis and Characterization of a Nano-hoop [c2]Daisy Chain Rotaxane. *Chem. Eur. J.* **2020**, *26*, 10205–10209. [[CrossRef](#)] [[PubMed](#)]
55. Cai, K.; Shi, Y.; Zhuang, G.; Zhang, L.; Qiu, Y.; Shen, D.; Chen, H.; Jiao, Y.; Wu, H.; Cheng, C.; et al. Molecular-Pump-Enabled Synthesis of a Daisy Chain Polymer. *J. Am. Chem. Soc.* **2020**, *142*, 10308–10313. [[CrossRef](#)] [[PubMed](#)]
56. Schroder, H.V.; Zhang, Y.; Link, A.J. Dynamic covalent self-assembly of mechanically interlocked molecules solely made from peptides. *Nat. Chem.* **2021**, *13*, 850–857. [[CrossRef](#)] [[PubMed](#)]
57. Tsuda, S.; Komai, Y.; Fujiwara, S.; Nishiyama, Y. Cyclodextrin-Based [c2]Daisy Chain Rotaxane Insulating Two Diarylacetylene Cores. *Chem. Eur. J.* **2021**, *27*, 1966–1969. [[CrossRef](#)]
58. Chu, C.; Stares, D.L.; Schalley, C.A. Light-controlled interconversion between a [c2]daisy chain and a lasso-type pseudo[1]rotaxane. *Chem. Commun.* **2021**, *57*, 12317–12320. [[CrossRef](#)]
59. Nhien, P.Q.; Tien, J.H.; Cuc, T.T.K.; Khang, T.M.; Trung, N.T.; Wu, C.H.; Hue, B.T.B.; Judy, I.W.; Lin, H.C. Reversible fluorescence and Förster resonance energy transfer switching behaviours of bistable photo-switchable [c2] daisy chain rotaxanes and photo-patterning applications. *J. Mater. Chem. C* **2022**, *10*, 18241–18257. [[CrossRef](#)]
60. Saura-Sanmartin, A.; Pastor, A.; Martinez-Cuezva, A.; Berna, J. Maximizing the [c2]daisy chain to lasso ratio through competitive self-templating clipping reactions. *Chem. Commun.* **2022**, *58*, 290–293. [[CrossRef](#)]
61. Trung, N.T.; Nhien, P.Q.; Kim Cuc, T.T.; Wu, C.; Buu Hue, B.T.; Wu, J.I.; Li, Y.; Lin, H. Controllable Aggregation-Induced Emission and Förster Resonance Energy Transfer Behaviors of Bistable [c2]Daisy Chain Rotaxanes for White-Light Emission and Temperature-Sensing Applications. *ACS Appl. Mater. Interfaces* **2023**, *15*, 15353–15366. [[CrossRef](#)] [[PubMed](#)]
62. Saura-Sanmartin, A.; Schalley, C.A. The Mobility of Homomeric Lasso- and Daisy Chain-Like Rotaxanes in Solution and in the Gas Phase as a means to Study Structure and Switching Behaviour. *Isr. J. Chem.* **2023**, *63*, e202300022. [[CrossRef](#)]
63. Clark, P.G.; Day, M.W.; Grubbs, R.H. Switching and Extension of a [c2]Daisy-Chain Dimer Polymer. *J. Am. Chem. Soc.* **2009**, *131*, 13631–13633. [[CrossRef](#)] [[PubMed](#)]
64. Du, G.; Moulin, E.; Jouault, N.; Buhler, E.; Giuseppone, N. Muscle-like Supramolecular Polymers: Integrated Motion from Thousands of Molecular Machines. *Angew. Chem.* **2012**, *51*, 12504–12508. [[CrossRef](#)] [[PubMed](#)]
65. Gao, L.; Zhang, Z.; Zheng, B.; Huang, F. Construction of muscle-like metallo-supramolecular polymers from a pillar[5]arene-based [c2]daisy chain. *Polym. Chem.* **2014**, *5*, 5734–5739. [[CrossRef](#)]
66. Fu, X.; Gu, R.R.; Zhang, Q.; Rao, S.J.; Zheng, X.L.; Qu, D.H.; Tian, H. Phototriggered supramolecular polymerization of a [c2]daisy chain rotaxane. *Polym. Chem.* **2016**, *7*, 2166–2170. [[CrossRef](#)]
67. Goujon, A.; Mariani, G.; Lang, T.; Moulin, E.; Rawiso, M.; Buhler, E.; Giuseppone, E. Controlled Sol–Gel Transitions by Actuating Molecular Machine Based Supramolecular Polymers. *J. Am. Chem. Soc.* **2017**, *139*, 4923–4928. [[CrossRef](#)]
68. Goujon, A.; Lang, T.; Mariani, G.; Moulin, E.; Fuks, G.; Raya, J.; Buhler, E.; Giuseppone, N. Bistable [c2] Daisy Chain Rotaxanes as Reversible Muscle-like Actuators in Mechanically Active Gel. *J. Am. Chem. Soc.* **2017**, *139*, 14825–14828. [[CrossRef](#)]
69. Goujon, A.; Moulin, E.; Fuks, G.; Giuseppone, N. [c2]Daisy chain rotaxanes as molecular muscles. *CCS Chem.* **2019**, *1*, 83–96. [[CrossRef](#)]
70. Zhang, Z.; You, W.; Li, P.; Zhao, J.; Guo, Z.; Xu, T.; Chen, J.; Yu, W.; Yan, X. Insights into the Correlation of Microscopic Motions of [c2]Daisy Chains with Macroscopic Mechanical Performance for Mechanically Interlocked Networks. *J. Am. Chem. Soc.* **2023**, *145*, 567–578. [[CrossRef](#)]
71. Hmadeh, M.; Fang, L.; Trabolsi, A.; Elhabiri, M.; Albrecht-Gary, A.M.; Stoddart, J.F. On the thermodynamic and kinetic investigations of a [c2]daisy chain polymer. *J. Mater. Chem.* **2010**, *20*, 3422–3430. [[CrossRef](#)]
72. Fu, G.C.; Nguyen, S.T.; Grubbs, R.H. Catalytic ring-closing metathesis of functionalized dienes by a ruthenium carbene complex. *J. Am. Chem. Soc.* **1993**, *115*, 9856–9857. [[CrossRef](#)]

73. Fox, H.H.; Schrock, R.R.; O'Dell, R. Coupling of Terminal Olefins by Molybdenum(VI) Imido Alkylidene Complexes. *Organometallics* **1994**, *13*, 635–639. [[CrossRef](#)]
74. Miller, S.J.; Grubbs, R.H. Synthesis of Conformationally Restricted Amino Acids and Peptides Employing Olefin Metathesis. *J. Am. Chem. Soc.* **1995**, *117*, 5855–5856. [[CrossRef](#)]
75. Hoveyda, A.H.; Zhugralin, A.R. The remarkable metal-catalysed olefin metathesis reaction. *Nature* **2007**, *450*, 243–251. [[CrossRef](#)]
76. Kumaraswamy, G.; Sadaiah, K.; Ramakrishna, D.S.; Police, N.; Sridhar, B.; Bharatam, J. Highly enantioselective carbon-carbon bond formation by Cu-catalyzed asymmetric [2,3]-sigmatropic rearrangement: Application to the syntheses of seven-membered oxacycles and six-membered carbocycles. *Chem. Commun.* **2008**, *42*, 5324–5326. [[CrossRef](#)]
77. Reddy, K.K.S.; Rao, B.V.; Raju, S.S. A common approach to pyrrolizidine and indolizidine alkaloids; formal synthesis of (-)-isoretronecanol, (-)-trachelanthamidine and an approach to the synthesis of (-)-5-epitashiromine and (-)-tashiromine. *Tetrahedron Asymmetry* **2011**, *22*, 662–668. [[CrossRef](#)]
78. Rao, G.B.D.; Anjaneyulu, B.; Kaushik, M.P. Greener and expeditious one-pot synthesis of dihydropyrimidinone derivatives using non-commercial β -ketoesters via the Biginelli reaction. *RSC Adv.* **2014**, *4*, 43321–43325. [[CrossRef](#)]
79. Rao, G.B.D.; Anjaneyulu, B.; Kaushik, M.P. A facile one-pot five-component synthesis of glycoside annulated dihydropyrimidinone derivatives with 1,2,3-triazol linkage via transesterification/Biginelli/click reactions in aqueous medium. *Tetrahedron Lett.* **2014**, *55*, 19–22. [[CrossRef](#)]
80. Bendi, A.; Rao, G.B.D. Strategic One-pot Synthesis of Glycosyl Annulated Phosphorylated/Thiophosphorylated 1,2,3-Triazole Derivatives Using CuFe_2O_4 Nanoparticles as Heterogeneous Catalyst, their DFT and Molecular Docking Studies as Triazole Fungicides. *Lett. Org. Chem.* **2023**, *20*, 568–578. [[CrossRef](#)]
81. Okay, O.; Reddy, S.K.; Bowman, C.N. Molecular Weight Development during Thiol-Ene Photopolymerizations. *Macromolecules* **2005**, *38*, 4501–4511. [[CrossRef](#)]
82. Sumerlin, B.S.; Vogt, A.P. Macromolecular Engineering through Click Chemistry and Other Efficient Transformations. *Macromolecules* **2010**, *43*, 1–13. [[CrossRef](#)]
83. Mazzolini, J.; Boyron, O.; Monteil, V.; Gignes, D.; Bertin, D.; D'Agosto, F.; Boisson, C. Polyethylene End Functionalization Using Radical-Mediated Thiol-Ene Chemistry: Use of Polyethylenes Containing Alkene End Functionality. *Macromolecules* **2011**, *44*, 3381–3387. [[CrossRef](#)]
84. Yokochi, H.; Ohira, M.; Oka, M.; Honda, S.; Li, X.; Aoki, D.; Otsuka, H. Topology Transformation toward Cyclic, Figure-Eight-Shaped, and Cross-Linked Polymers Based on the Dynamic Behavior of a Bis(hindered amino)disulfide Linker. *Macromolecules* **2021**, *54*, 9992–10000. [[CrossRef](#)]
85. Nomura, T.; Onimura, K.; Yamabuki, K. Synthesis and Polymerization of Acid-degradable Rotaxane Using Boc Protecting Group. *Chem. Lett.* **2022**, *51*, 16–19. [[CrossRef](#)]
86. Moeller, N.; Ruehling, A.; Lamping, S.; Hellwig, T.; Fallnich, C.; Ravoo, B.J.; Glorius, F. Stabilization of High Oxidation State Upconversion Nanoparticles by N-Heterocyclic Carbenes. *Angew. Chem. Int. Ed.* **2017**, *56*, 4356–4360. [[CrossRef](#)]
87. Liu, D.; Wang, D.; Wang, M.; Zheng, Y.; Koynov, K.; Auernhammer, G.K.; Butt, H.; Ikeda, T. Supramolecular Organogel Based on Crown Ether and Secondary Ammoniumion Functionalized Glycidyl Triazole Polymers. *Macromolecules* **2013**, *46*, 4617–4625. [[CrossRef](#)]

Disclaimer/Publisher's Note: The statements, opinions and data contained in all publications are solely those of the individual author(s) and contributor(s) and not of MDPI and/or the editor(s). MDPI and/or the editor(s) disclaim responsibility for any injury to people or property resulting from any ideas, methods, instructions or products referred to in the content.